Article

Study on the Reaction Mechanism of Ethylene Propylene Diene Monomer Sealing Material and $C_5F_{10}O-CO_2$ Gas Mixture

Yalong Li, Xiaoxing Zhang,* Cheng Xie, Zhuo Wei, Song Xiao, and Ju Tang

Read Online

ACCESS | Metrics & More | Article Recommendations

ABSTRACT: The eco-friendly insulating medium $C_5F_{10}O$ gas has attracted the attention of many researchers due to its superior environmental protection and insulation properties. However, there are few studies on the compatibility of $C_5F_{10}O$ gas with sealing materials for the gas-insulated equipment (GIE), which will bury hidden dangers for its engineering application. In this study, the compatibility of $C_5F_{10}O$ gas with an ethylene propylene diene monomer (EPDM) sealing material which is most used in equipment was tested, and its reaction mechanism was simulated. The study found that the O element on the carbonyl group of $C_5F_{10}O$ gas has high chemical reactivity and will interact with EPDM rubber. During the interaction process, EPDM rubber will also react with the C_3F_6 gas generated by the decomposition of $C_5F_{10}O$ gas, and at the same time, it will also decompose $C_5F_{10}O$ gas to produce more C_3F_6O and C_3HF_7. The surface of EPDM rubber will produce oily substances and a large number of crystal particles, which will cause its mechanical properties to deteriorate and shorten its service life. Therefore, it is necessary to carry out anti-corrosion treatment on the surface of EPDM rubber or replace the sealing material with better compatibility when designing and manufacturing GIE.
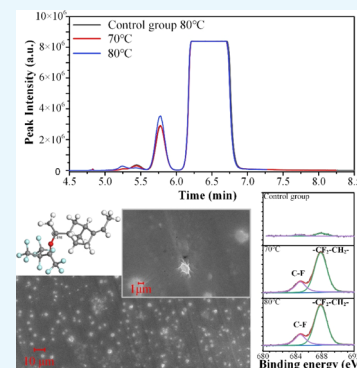
1. INTRODUCTION

Sulfur hexafluoride (SF_6) gas has been widely used in the gas-insulated equipment (GIE) of power systems due to its excellent insulation and arc extinguishing performance.[1] However, SF_6 gas has a very high greenhouse effect. Its global warming potential (GWP) is 23,500 times that of CO_2, and its life span in the atmosphere is about 3200 years.[2] As early as 1997, the "Kyoto Protocol" clearly listed it as a greenhouse gas that needs to be restricted.[3,4] The "Paris Agreement" signed at the end of 2015 also pointed out that countries in the world should strive to achieve net-zero emissions of greenhouse gases by the end of this century while keeping the global warming value within 1.5−2%.[5] In response to the global call for energy conservation and emission reduction, avoiding the greenhouse effect caused by the use of SF_6 gas and realizing the green and sustainable development of the power industry, it has become a research hotspot in related fields to find environmentally friendly insulating media for power systems.[6]

The excellent insulation properties of $C_5F_{10}O$ (1,1,1,3,4,4,4-heptafluoro-3-(trifluoromethyl)-2-butanone) gas have received extensive attention from many researchers in recent years.[7] The insulation performance of pure $C_5F_{10}O$ gas is about 1.4 times that of SF_6 gas, its GWP value is less than 1 (equivalent to CO_2), and its atmospheric lifetime is only 15 days. However, the liquefaction temperature of $C_5F_{10}O$ gas of 26.9 °C under normal pressure limits its application. In engineering applications, pure $C_5F_{10}O$ gas cannot be used alone as an insulating medium. It must be mixed with low-boiling buffer

gases (such as N_2, synthetic air, CO_2, and so forth) to meet the requirements for liquefaction temperature in engineering practice.[8]

Currently, many researchers have carried out a lot of research on the physical and chemical properties,[9,10] insulation properties,[11] decomposition characteristics,[12,13] and arc extinguishing characteristics[14] of $C_5F_{10}O$ and its gas mixture and have achieved certain results, confirming that the $C_5F_{10}O$ gas mixture has the potential to be used in various medium- and low-voltage GIE. It is necessary to carry out the compatibility study of $C_5F_{10}O$ gas and the internal materials of the equipment before engineering applications. $C_5F_{10}O$ gas will be in direct contact with the internal materials of GIE, so it is required that $C_5F_{10}O$ gas and the internal materials of GIE can coexist for a long time and have good compatibility. Kessler *et al.* had carried out accelerated aging experiments of $C_5F_{10}O$ gas and materials such as metals, alloys, and insulators inside GIE within the range of 75−225 °C. Studies had shown that $C_5F_{10}O$ gas and metals are still stable at high temperatures, whereas $C_5F_{10}O$ gas will react with insulators or elastomers to

produce C_3HF_7 and C_3F_6.[15] Zhang *et al.* first studied the interaction mechanism between $C_5F_{10}O$ and metal materials in electrical equipment through density functional theory (DFT). The calculation found that the oxygen atom in the $C_5F_{10}O$ molecule has a strong interaction force with the Cu(1 1 1) surface, while the fluorine atom has a weak interaction force with the Cu(1 1 1) surface, which belongs to physical adsorption.[16] The interaction force between $C_5F_{10}O$ molecule and Al(1 1 1) is stronger than that of Ag(1 1 1), which belongs to chemical adsorption, and the interaction mechanism between the $C_5F_{10}O$ molecule and Ag(1 1 1) is physical interaction.[17] Experimental research on the compatibility of the $C_5F_{10}O-CO_2$ gas mixture with metal materials copper and aluminum had shown that the compatibility of copper and the $C_5F_{10}O-CO_2$ gas mixture is significantly lower than that of aluminum. The interaction between the $C_5F_{10}O-CO_2$ gas mixture and copper at the temperature above 100 °C for 8 h will corrode the copper surface and form cubic grains, but there is no corrosion on the aluminum surface.[6] Experimental research on the compatibility of $C_5F_{10}O-N_2$ and $C_5F_{10}O-$ synthetic air gas mixtures with metal material copper had shown that oxygen at high temperatures will aggravate the corrosion of $C_5F_{10}O$ gas on the copper surface. Therefore, it is necessary to protect the copper contacts inside GIE with silver plating to prevent $C_5F_{10}O$ gas from corroding the copper surface.[18]

$C_5F_{10}O$ gas is a new synthetic gas. It is an indispensable step to study the compatibility of $C_5F_{10}O$ gas with internal materials of GIE before engineering applications. Relevant researchers have conducted studies on the metal materials (copper, aluminum, and silver) used in GIE, but there are few reports on the compatibility of rubber sealing materials used in GIE with $C_5F_{10}O$ gas. If the compatibility of $C_5F_{10}O$ gas and rubber sealing materials is poor, it will lead to accelerated aging of the sealing materials, shortened service life, and increased annual leakage rate and even cause equipment insulation breakdown due to gas leakage. Therefore, study on the compatibility of $C_5F_{10}O$ gas and rubber sealing materials will have guiding significance for its engineering applications.

In this study, a $C_5F_{10}O$ gas and rubber sealing material compatibility test platform was built, and ethylene propylene diene monomer (EPDM) rubber seal ring, the most commonly used sealing material in GIE, was used as the test object. The compatibility of the $C_5F_{10}O-CO_2$ gas mixture and EPDM rubber was studied by the thermal acceleration test.

2. RESULTS AND ANALYSIS

When using GCMS to detect the components of the gas mixture, first, one should use the SCAN mode to scan all possible decomposition products. The chromatographic peaks of the decomposition products are shown in Figure 1a. The mass-to-charge ratios (m/z) of $C_5F_{10}O$ gas and decomposition products are shown in Table 1. The decomposition products were found to be C_3F_6O, C_3F_6, and C_3HF_7 through mass spectrometry identification. The reasons why the decomposition products of the control test group contained H-containing C_3HF_7 are as follows: In the test process of this research, the impurity inside the gas chamber was removed by vacuuming and using pure CO_2 gas to clean the gas chamber, which avoided the interference of impurity gas to the greatest extent, but there were still traces of H_2O remaining on the inside and inner wall of the gas chamber, and it participates in the decomposition reaction of $C_5F_{10}O$ gas during the test. The
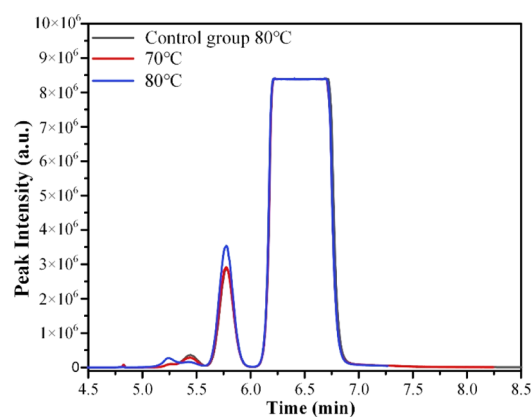
(a)
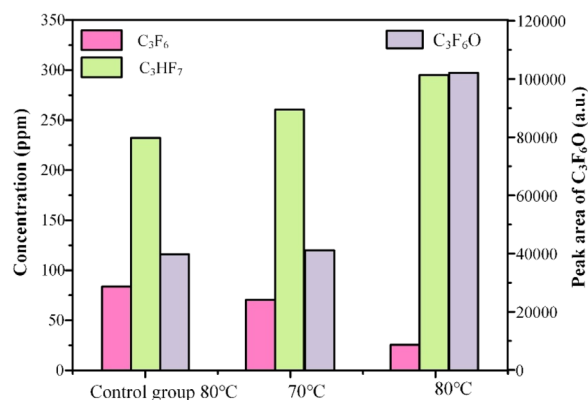
(b)

Figure 1. Decomposition products of the $C_5F_{10}O-CO_2$ gas mixture and EPDM rubber after thermal aging. (a) Qualitative analysis of decomposition products of $C_5F_{10}O$ gas. (b) Quantitative analysis results of decomposition products of $C_5F_{10}O$ gas.

Table 1. $C_5F_{10}O$ Gas and Its Decomposition Product Mass-to-Charge Ratios (m/z) and Separation Time

gas type	mass-to-charge ratios (m/z)	separation time (min)
$C_5F_{10}O$	69, 97, 169, 197, 266	6.04−6.90
C_3F_7H	69, 151	5.55−6.01
C_3F_6	69, 100, 131, 150	5.27−5.61
C_3F_6O	50, 69, 119	4.97−5.56

safety data sheet of $C_5F_{10}O$ gas shows that $C_5F_{10}O$ reacts with water by violent hydrolysis, and the rate of reaction with water is fast at room temperature, and the half-life of hydrolysis is about 11.5 min.[7] In the reaction process, H_2O will decompose to produce $H^\bullet$ and $OH^\bullet$ and react with $CF_3^\bullet$, $C_3F_7^\bullet$, and $F^\bullet$ particles generated by the decomposition of $C_5F_{10}O$ gas and finally generate decomposition products such as C_3F_6 and C_3HF_7.[13,14] From the chromatogram of the control group shown in Figure 1a, it can be seen that the $C_5F_{10}O-CO_2$ gas mixture will react with the stainless steel shell outside the heat source at high temperatures and produce three decomposition products of C_3F_6O, C_3F_6, and C_3HF_7. In the test group, the main decomposition products produced by the contact of the $C_5F_{10}O-CO_2$ gas mixture with EPDM are also three decomposition products of C_3F_6O, C_3F_6, and C_3HF_7. The difference is that the concentrations of the three decomposition products produced by them are different.

In order to study the effect of EPDM on the decomposition products of $C_5F_{10}O$ gas under different temperature conditions, C_3F_6 and C_3HF_7 were quantitatively studied using C_3F_6 and C_3HF_7 standard concentration gases. Since the standard concentration of C_3F_6O gas cannot be obtained temporarily, the peak area of C_3F_6O gas produced by different test groups can be obtained by integrating the mass spectrum peak area with the m/z of 119 in C_3F_6O gas, and the concentration change of C_3F_6O gas can be studied by comparing the peak area in a semi-quantitative way. The quantitative analysis diagrams of the three decomposition products of C_3F_6O, C_3F_6, and C_3HF_7 are shown in Figure 1b.

When the test temperature was 80 °C, the EPDM test group produced more C_3F_6O and C_3HF_7 than the $C_5F_{10}O$ gas decomposition in the control group, while the content of C_3F_6 was greatly reduced. The concentrations of C_3F_6 and C_3HF_7 produced by the control test group were 83.70 and 232.33 ppm, respectively. The concentration of C_3F_6 produced by the 80 °C EPDM rubber test group decreased by 69.57%, and the concentration of C_3F_6O and C_3HF_7 increased by 156.55 and 26.98%, respectively. In the different temperature test groups, the concentrations of C_3F_6 and C_3HF_7 produced by the decomposition of the test group at 70 °C were 70.45 and 260.38 ppm, respectively, and the concentration of C_3F_6 produced by the EPDM rubber test group at 80 °C decreased by 64.41%, whereas the concentration of C_3F_6O and C_3HF_7 increased by 148.09 and 13.30%, respectively. The above results indicate that long-term contact between $C_5F_{10}O$ gas and the surface of the stainless steel shell outside the heat source will decompose the trace of $C_5F_{10}O$ gas and produce three main decomposition products: C_3F_6O, C_3F_6, and C_3HF_7.

After the test is over, the gas inside the gas chamber is extracted through the exhaust gas collection and recovery system, and the sample of the EPDM rubber sealing ring taken out is shown in Figure 2. From left to right, there are samples

Figure 2. Surface photos of EPDM rubber before and after the test.

of EPDM rubber sealing rings before the test and when the test temperature is 70 and 80 °C, respectively. The EPDM rubber before the test showed a black matt appearance, and the rubber surface after the test had a layer of oily substance attached to the surface. In order to further explore the surface changes of EPDM rubber in contact with $C_5F_{10}O$ gas under thermal aging conditions, it is necessary to characterize EPDM rubber samples before and after the test to reveal their interaction mechanism.

3. CHARACTERIZATION OF EPDM SAMPLES AND THEIR INTERACTION MECHANISM

3.1. Rubber Tensile Test. The EPDM rubber sealing rings used in this study are the O-type rubber ring used in the GIE produced by the XJ Group and not the standard test rubber sample. One should refer to the rubber tensile standard test principle; the length of the tensile test sample is 65 mm and the tensile speed is 500 mm/min.[19] The tensile stress and strain properties of EPDM rubber samples before and after the test are shown in Figure 3 and Table 2. The elongation at
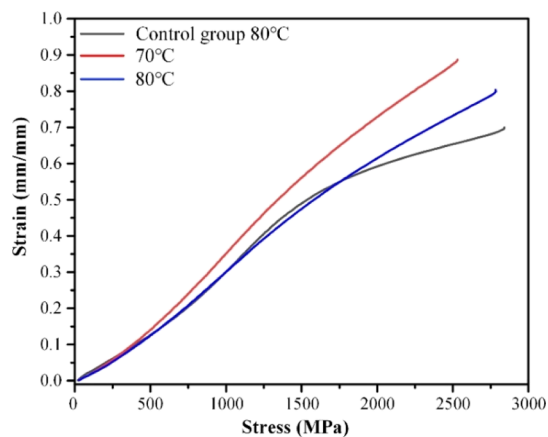
Figure 3. Tensile stress−strain curve of EPDM rubber samples before and after the test.

Table 2. Elongation at Break and Maximum Force of EPDM Rubber Samples

	elongation at break (%)	maximum force (MPa)
control group	111.60	250.00
70 °C test group	89.87	222.78
80 °C test group	92.65	245.18

break of the EPDM rubber sample before the test was 111.60%, and the maximum tensile force was 250.00 MPa. However, the elongation at break of the EPDM sample at 70 and 80 °C was reduced by 19.47 and 16.98%, and the maximum tensile force was reduced by 10.88 and 1.92%, respectively. The changes in mechanical parameters indicate that the EPDM rubber has embrittled, and the mechanical properties of EPDM rubber samples are slightly reduced after the thermal aging test.

3.2. SEM Test. Figure 4 shows the changes in the surface morphology of EPDM rubber before and after the test. The EPDM rubber before the test had some small ravines on the surface. Under high magnification, it can be observed that the surface of the rubber is covered with grit-like particles. These phenomena are caused by the rubber manufacturing process. When the test temperature is 70 °C, the small ravines on the surface of EPDM rubber are not as obvious as those in the control group. Most of the grit-like particles observed under high magnification have disappeared. Except for the precipitation of crystal particles (white particles in the picture) in some areas, the surface of the rubber has a relatively smooth morphology. The above results show that when the test temperature is 70 °C, the EPDM rubber has begun to appear slightly corroded after being thermally aged for 90 h in the $C_5F_{10}O−CO_2$ gas mixture. When the test temperature is 80
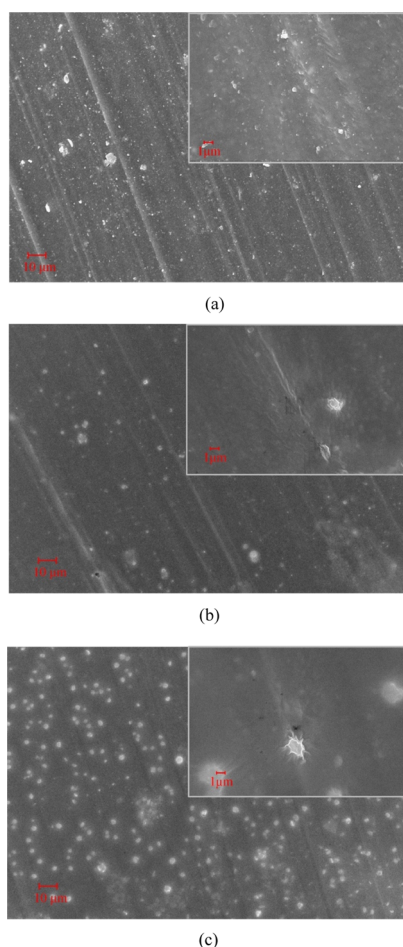
Figure 4. Surface morphology of EPDM rubber before and after the test. (a) Control group. (b) 70 °C test group. (c) 80 °C test group.

°C, a large number of crystal particles are uniformly distributed on the surface of EPDM rubber, indicating that the structure of the rubber surface has been severely damaged and a large number of crystal particles are exposed. The crystal particles on the rubber surface come from the crosslinking agent added during the production of EPDM rubber and precipitated to the surface due to high temperature.

3.3. XPS Test. The EPDM rubber is a kind of copolymer formed by ethylene, propylene, and a small amount of non-conjugated diene. The chemical elements are mainly C and H elements. Since the photoionization interface of the H and He elements is small and the signal is too weak, XPS cannot detect these two elements, so the change of the H element is not considered. In order to further study the change law of elements (F 1s, C 1s, and O 1s) on the surface of EPDM rubber samples, this study used XPS to perform energy spectrum scanning tests (the orbits of the tested elements are selected according to the international general test rules) on the elements that may exist on the rubber surface. We first use XPS Peak software to perform a Shirley-type fitting deduction on the background of the energy spectrum and then use the Gaussian algorithm to perform peak fitting.[20] Finally, refer to the National Institute of Standards and Technology XPS database and previous studies[21] to determine the chemical state, molecular structure, and chemical bonds of the elements. The results are shown in Table 3 and Figure 5.

Table 3. Changes in Surface Element Content of EPDM Rubber Samples before and after the Test

	C (%)	F (%)	O (%)
control group	79.13	1.18	19.69
70 °C test group	65.16	15.37	19.47
80 °C test group	64.24	17.46	18.30

From the changes of the elements on the surface of EPDM rubber samples before and after the test listed in Table 3, it can be seen that the content of the C element on the surface of the rubber samples is the highest, and its proportion of the surface of the EPDM rubber sample before the test is close to 80%. The reason that the rubber surface before the test contained 19.69% of the O element was that EPDM rubber was vulcanized with peroxide as a cross-linking agent to obtain more excellent mechanical and insulating properties, so its surface contained the O element. During the heat aging test, the proportion of O element decreased slightly, and the higher the test temperature, the more the proportion of the O element on the rubber surface decreased. This is due to the large increase in the content of the F element during the thermal aging test, which indirectly caused the relative decrease in the proportion of C and O. The increase in the content of the F element also indirectly indicates that $C_5F_{10}O$ gas interacts with EPDM rubber during the thermal aging process.

From the high-resolution photoelectron spectra of F 1s, C 1s, and O 1s shown in Figure 5, it can be seen that the characteristic chemical bonds of the elements on the surface of EPDM rubber samples have changed after the test. The different characteristic chemical bonds' information in the figure represents different material characteristics, which directly indicates that $C_5F_{10}O$ gas interacts with EPDM rubber during the high-temperature thermal aging process. Figure 5a shows the photoelectron spectrum of the F 1s orbital on the surface of the rubber samples. The EPDM rubber before the test did not contain the F element, and the surface of the rubber after the test detected two characteristic peaks of the F element. The C−F bond and the $-CF_2-CH_2-$ group were detected at 684.50 and 688.15 eV, respectively. The C−F bond at 684.50 eV indicates that the chemical bond formed by the F atom fixed to the C atom was detected on the rubber surface.[22] The reason may be that $C_5F_{10}O$ gas or its decomposition product gas detected above was attached to the rubber surface. However, the $-CF_2-CH_2-$ group confirmed that the $-CF_2-$ group replaced the $-CH_2-$ group in the rubber during the reaction of $C_5F_{10}O$ gas with rubber and formed a long-chain structure containing organic fluorine groups. The photoelectron spectroscopy of the C 1s orbital on the surface of the rubber samples shown in Figure 5b detected the chemical bond formed by the C and O elements, which is a characteristic peak of the peroxide crosslinker. It is important to point out that the C element on the surface of EPDM rubber samples produced a new characteristic peak at 292.80 eV after the test, which corresponds to the $-CF_2-CF_2-$ group. This is also consistent with the detection result of the F element shown in Figure 5a. Combined with the previous test results that the concentration of C_3F_6 produced by the decomposition of $C_5F_{10}O$ is lower than that of the control group, it is shown that the $-CF_2-CF_2-$ groups detected in Figure 5a,b are mainly produced by the reaction of C_3F_6 with EPDM. Although the photoelectron spectroscopy of the O 1s orbital on the surface of the rubber sample shown in Figure 5c
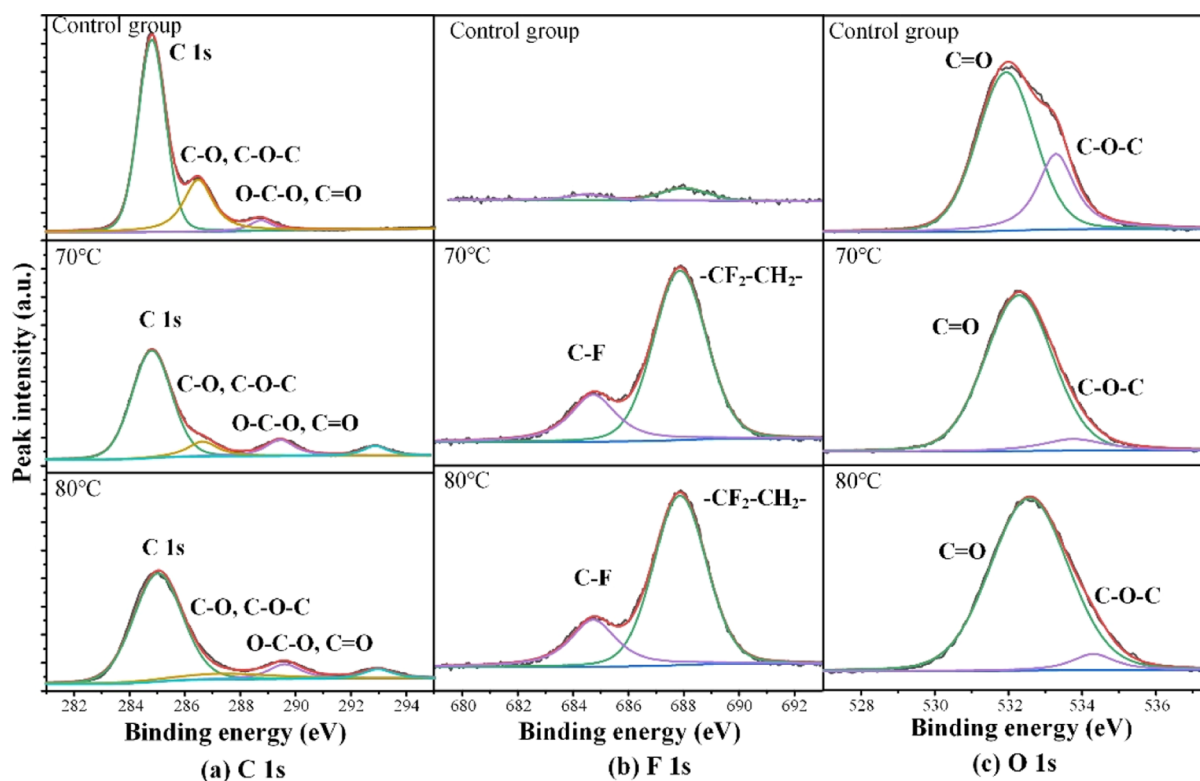
Figure 5. Surface element analysis of EPDM rubber before and after the test.

did not detect the formation of new characteristic chemical bonds, the two characteristic peak intensities of the O element also changed to varying degrees before and after the test.

The new characteristic peaks of F 1s and C 1s in the above results confirm that $C_5F_{10}O$ gas and EPDM rubber have a chemical reaction under thermal aging conditions, and $C_5F_{10}O$ gas will corrode the surface of EPDM rubber at high temperatures.

3.4. Reaction Mechanism of $C_5F_{10}O$ and EPDM. In order to analyze the interaction mechanism between $C_5F_{10}O$ gas and EPDM, density functional theory (DFT) was used. EPDM rubber is a copolymer formed of ethylene, propylene, and a small amount of non-conjugated diene. Ethylene norbornene is usually used as the diene. Its main advantages are fast vulcanization speed and high vulcanization efficiency. In this study, the ethylene−propylene−ethylidene norbornene chain was selected as the model of EDPM rubber for DFT calculation. Yamada *et al.* also used this scheme to study the interaction mechanism between nitrile rubber and fuel species based on DFT.[23] EPDM defects and particles have unsaturated chemical bonds and are more reactive than EPDM molecules. Therefore, the reaction between $C_5F_{10}O$ and EPDM defects or particles can occur more easily than EPDM molecules.[21] We used the Perdew−Burke−Ernzerhof-generalized gradient approximation method in our calculations to deal with electronic exchange and correlation.[24] In the calculations, the double numerical plus polarization was used to add polarization functions to all atoms, and all electrons were processed using all electrons relativistically, and the relativistic effect was introduced in the processing of core electrons to make the calculation results more accurate and reliable.[25] The convergence tolerance settings in the geometric optimization calculation process are as follows: 1.0×10^{-6} Ha for energy,

(2) 0.005 Å for maximum displacement, and (3) 0.002 Ha/Å for maximum force.[21]

The reaction enthalpy of a chemical reaction is defined as follows:

$$\text{enthalpy} = E_{\text{product}} - E_{\text{reactant}} \quad (1)$$

where the negative value of the reaction enthalpy indicates that the reaction is thermodynamically spontaneous and the positive value of the reaction enthalpy indicates that the reaction is an endothermic process.

Because the EPDM molecule is a complex organic macromolecular structure, the interaction mechanism between EPDM rubber and $C_5F_{10}O$ gas discussed in this study mainly focuses on the reaction of EPDM rubber defects or particles with $C_5F_{10}O$ molecules. The defects and particles of EPDM rubber have unsaturated chemical bonds, and its chemical reaction activity is higher than that of EPDM rubber molecules. In other words, the reaction between $C_5F_{10}O$ molecules and EPDM defects and particles is more likely to occur than EPDM molecules. The structure of the EPDM monomer is shown in Figure 6a. From its structural characteristics, it can be found that there were four possible defect formation paths for EPDM rubber (marked by the arrow in the figure).

The energy barrier and reaction enthalpy required by EPDM rubber to form the four defect paths are shown in Figure 6b−e. EPDM rubber requires 108.80 kcal/mol of energy to form defects through the process of the chemical bond breaking shown in reaction path 1, and the reaction enthalpy is 90.99 kcal/mol. EPDM rubber requires 184.74 kcal/mol of energy to form defects through the process of the chemical bond breaking shown in reaction path 2, and the reaction enthalpy is 89.18 kcal/mol. EPDM rubber requires 234.94 kcal/mol of energy to form defects through the process of the chemical
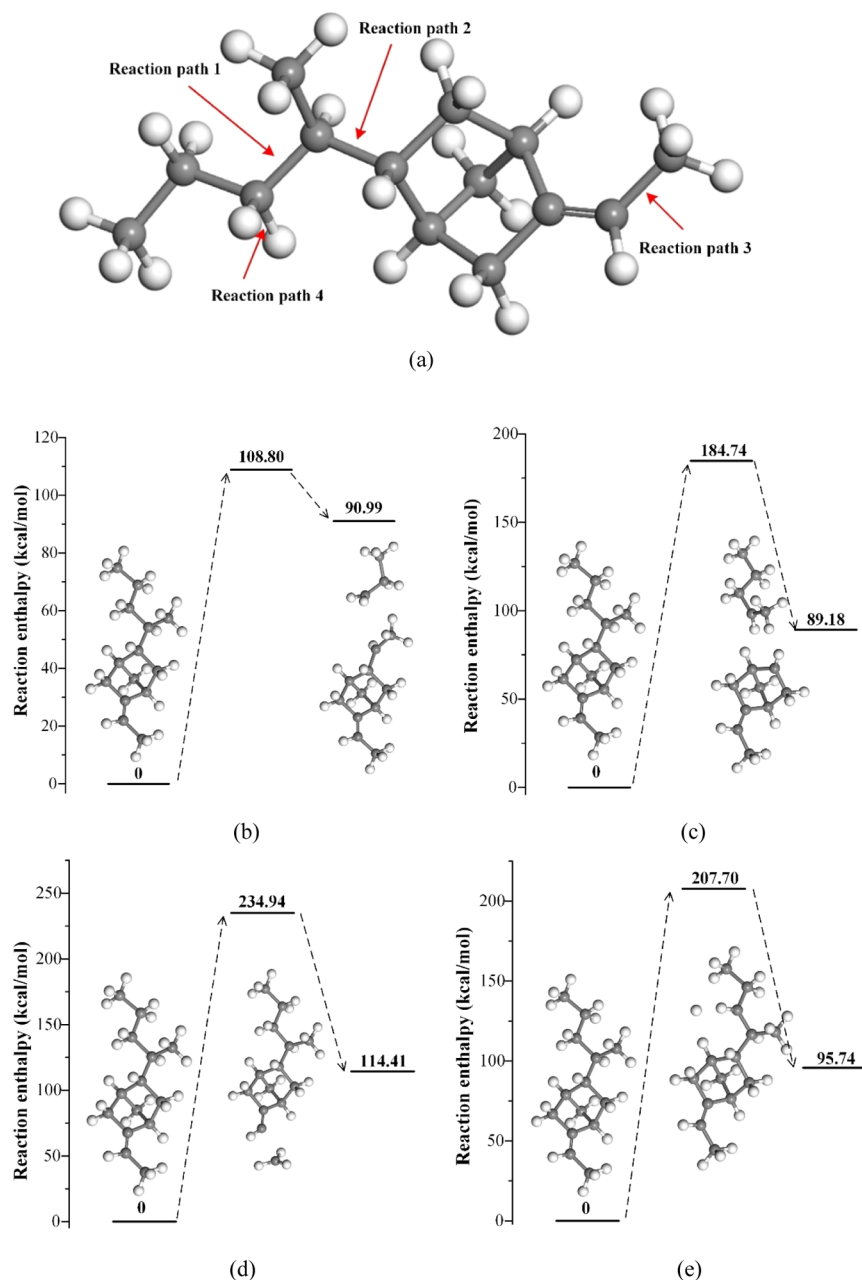
Figure 6. Enthalpy of reaction formed by defects in EPDM rubber. (a) Monomer structure and defect formation path of EPDM. (b) Reaction path 1. (c) Reaction path 2. (d) Reaction path 3. (e) Reaction path 4.

bond breaking shown in reaction path 3, and the reaction enthalpy is 114.41 kcal/mol. EPDM rubber requires 207.70 kcal/mol of energy to form defects through the process of the chemical bond breaking in the dehydrogenation process shown in reaction path 4, and the reaction enthalpy is 95.74 kcal/mol.

We calculated the possible interactions between the $C_5F_{10}O$ molecule and four kinds of EPDM defects and considered the structural characteristics of the $C_5F_{10}O$ molecule to construct the initial structure model of 24 possible reaction models. The calculation results show that C and F elements in the $C_5F_{10}O$ molecule have low chemical reactivity and cannot react with EPDM defects, while the O element in the $C_5F_{10}O$ molecule has high chemical reactivity and can react with EPDM defects to form chemical bonds. The adsorption models of the $C_5F_{10}O$ molecule and EPDM defects obtained by calculation are shown in Figure 7.

The eight types of defects formed in the four reaction paths shown in Figure 6b−e interact with the O element in the $C_5F_{10}O$ molecule to form eight adsorption models. When the O element in the $C_5F_{10}O$ molecule is close to the defects of EPDM rubber, the optimized structures show that the distance between the O in the $C_5F_{10}O$ molecule and the C element or the H element in the EPDM defect was shortened. When the O element in the $C_5F_{10}O$ molecule is close to the C element in the EPDM defect in paths 1−3, the optimized structures show that the distance between the O and C elements in the EPDM defect was about 1.500 Å, the distances between the O and C elements in the two EPDM defects in reaction path 3 were 1.456 and 1.377 Å, respectively, and the distance between O in the $C_5F_{10}O$ molecule and H elements in the EPDM defect in reaction path 4 was 0.979 Å.

Figure 7. Enthalpy of reaction between $C_5F_{10}O$ gas and defects in EPDM rubber.

In addition, the calculation results show that the enthalpy values of all reaction paths are negative, that is, the reaction process is exothermic. The reaction enthalpy of reaction paths 3A and 4B is significantly higher than that of the other six reaction paths (approximately −20.00 kcal/mol). Among them, path 3A with the largest reaction enthalpy value is −41.71 kcal/mol, and path 4A with the smallest reaction enthalpy value is −17.61 kcal/mol. The two adsorption models formed by reaction paths 3A and 4B have the largest reaction enthalpy and the most heat released during the adsorption process. Therefore, the two reaction paths are most likely to undergo adsorption reaction between $C_5F_{10}O$ molecules and EPDM defects. The chemical reaction that causes the fluorine element to accumulate on the rubber surface is also more likely to occur through the above two paths.

3.5. Discussion. According to the above results, the interaction between $C_5F_{10}O$ and EPDM rubber defects and particles will cause the adsorption of $C_5F_{10}O$ on the rubber surface. The O element in the carbonyl (C=O) group of $C_5F_{10}O$ is chemically active and can easily react with EPDM defects or particles to form chemical bonds. $C_5F_{10}O$ gas has poor compatibility with EPDM during high-temperature thermal aging. This shortcoming should be considered when designing and manufacturing GIE sealing materials. In order to prevent the corrosion of the sealing material from accelerating its aging process, resulting in the shortening of the service life of the equipment and even the insulation failure caused by gas leakage, we need to perform anti-corrosion treatment on the surface of EPDM rubber or use rubber with better compatibility with $C_5F_{10}O$ gas as a sealing material.

4. CONCLUSIONS

In this study, the EPDM rubber sealing ring used in GIE by State Grid XJ Group Co., Ltd. was used as the test object to explore the compatibility of $C_5F_{10}O$ gas and EPDM rubber under thermal aging. After the thermal aging test, the changes in gas composition, mechanical properties, surface morphology, and element changes of EPDM rubber were tested, the reaction mechanism was simulated, and the following conclusions were obtained:

(1) Under thermal aging conditions, minor amounts of $C_5F_{10}O$ gas will react with the outer shell of the stainless steel container to decompose and generate C_3F_6O, C_3F_6 and C_3HF_7. EPDM rubber will react with the C_3F_6 gas produced by the decomposition of $C_5F_{10}O$ gas, reducing the content of C_3F_6 in the decomposition products.

(2) During the thermal aging test, oily substances will be formed on the surface of EPDM rubber, and a large number of crystal particles will be observed on the surface under the microscopic view. This change will make EPDM rubber brittle and decrease the mechanical properties.

(3) The O element on the carbonyl group in the $C_5F_{10}O$ molecule has high reactivity and will form a stable adsorption structure and form new chemical bonds during the interaction process with EPDM rubber defects and particles.

(4) The reaction of EPDM and $C_5F_{10}O$ gas will accelerate its aging and shorten its service life. In the process of designing and manufacturing GIE, the surface of EPDM rubber should be treated with anti-corrosion or replaced with rubber with better compatibility.

5. EXPERIMENTAL SECTION

The test platform is shown in Figure 8, which is mainly composed of a heating system, a temperature feedback control
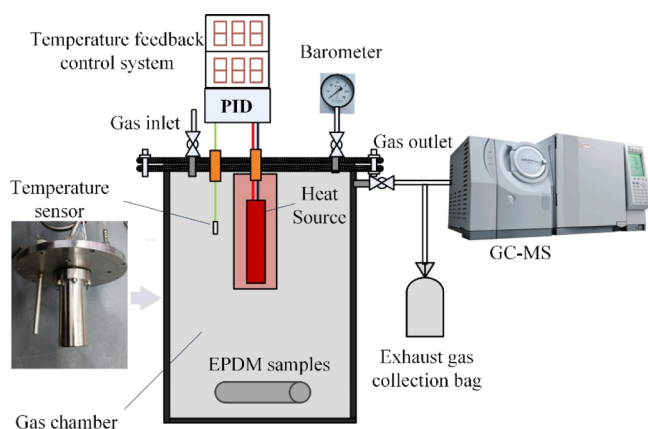
Figure 8. $C_5F_{10}O-CO_2$ gas mixture and EPDM rubber thermal acceleration test platform.

system, a detection system, and an exhaust gas collection and recovery system. The heating system includes a heat source and a 304 stainless steel shell outside the heat source. The heat source transfers heat to the surface through the stainless steel shell so that the gas is heated more uniformly. The outer wall of the gas chamber is also made of 304 stainless steel, which ensures that the gas chamber has high chemical stability. The temperature feedback monitoring and control system includes a temperature sensor and a proportion integration differentiation (PID) controller. The temperature sensor is used to monitor the temperature of the test gas and provide feedback of the temperature signal to the PID controller to control the test process. There is also a sensor for monitoring the gas temperature inside the gas chamber. The detection system includes a gas chromatograph—mass spectrometer, a field emission scanning electron microscope, and an X-ray photo-electron spectrometer. The gas chromatograph—mass spec-

trometer is the GCMS-QP2010 Ultra gas chromatography mass spectrometer produced by Shimadzu. The chromatographic column model is CP-SIL 5 CB, and the film thickness, length, and inner diameter of the chromatographic column are 8 μm, 60 m, and 0.32 mm, respectively. FESEM is produced by Carl Zeiss and is used to observe the changes in the surface morphology of EPDM rubber after heat aging. XPS is used to characterize the element composition, content, and characteristic chemical bonds of the EPDM rubber surface and can be used to analyze the chemical reactions that occur on the EPDM rubber surface.

The $C_5F_{10}O$ gas used in the test was provided by Minnesota Mining and Manufacturing (3M) with a purity of 99.5%, and high-purity CO_2 was provided by Wuhan Niuride Special Gas Co., Ltd. with a purity of 99.999%. The EPDM rubber material is the sample of the EPDM seal ring in GIE produced by State Grid XJ Group Co., Ltd. The sample is a cylindrical shape with a diameter of 5 mm. The cleaning steps of EPDM rubber samples before the test were as follows: first, we should put the EPDM rubber sample in distilled water and use ultrasonic cleaning for 1 h to remove the impurities on the surface to prevent it from affecting the test results, and then we should put the sample in a drying oven to dry for 24 h to remove water.

The gas used in the experiment of this research was a 7.5% $C_5F_{10}O-92.5\%$ CO_2 gas mixture (volume fraction). Since the gas pressure in the gas chamber will rise during the thermal aging process, the gas pressure was set to 0.2 MPa (relative pressure) for safety reasons. The relevant regulations stipulate that the maximum ambient temperature for the safe and stable operation of GIE is 40 °C, and the allowable upper limit of temperature rise of metal products can reach 65–75 °C.[6] EPDM is generally used as the sealing material of GIE, and the temperature of the equipment casing is usually lower. GB/T 11022-2011[26] stipulates that the maximum temperature rise of the part that can be touched in normal operation is 30 °C, and the maximum temperature rise of the part that does not need to be touched in normal operation is 40 °C. Therefore, considering the actual operating conditions of GIE, the test temperature was selected as 70 and 80 °C, and control groups with the temperature of 80 °C were set up. The control group had the same conditions as the test group except that no EPDM was placed. There is currently no compatibility test standard for non-SF_6 gas insulating media and rubber materials. In order to have sufficient reaction time between $C_5F_{10}O$ gas and EPDM rubber, the thermal aging test time was 90 h.[21] After the test, the gas sample in the gas chamber was collected and GCMS was used to detect the change in gas composition.

■ AUTHOR INFORMATION

Corresponding Author

Xiaoxing Zhang − School of Electrical Engineering and Automation, Wuhan University, Wuhan 430072, P. R. China; ◉ orcid.org/0000-0001-5872-2039; Phone: +86 13627275072; Email: xiaoxing.zhang@outlook.com

Authors

Yalong Li − School of Electrical Engineering and Automation, Wuhan University, Wuhan 430072, P. R. China

Cheng Xie − State Grid Zhejiang Electric Power Research Institute, Hangzhou 310007, P. R. China

Zhuo Wei − *School of Electrical Engineering and Automation, Wuhan University, Wuhan 430072, P. R. China*

Song Xiao − *School of Electrical Engineering and Automation, Wuhan University, Wuhan 430072, P. R. China*

Ju Tang − *School of Electrical Engineering and Automation, Wuhan University, Wuhan 430072, P. R. China*

Complete contact information is available at:
https://pubs.acs.org/10.1021/acsomega.1c03491

Notes
The authors declare no competing financial interest.

■ REFERENCES

(1) Xiao, S.; Gao, B.; Pang, X.; Zhang, X.; Li, Y.; Tian, S.; Tang, J.; Luo, Y. The sensitivity of C_4F_7N to electric field and its influence to environment-friendly insulating gas mixture C_4F_7N/CO_2. *J. Phys. D: Appl. Phys.* **2020**, *54*, 055501.

(2) Stocker, T. *Climate change 2013: The Physical Science Basis: Working Group I Contribution to the Fifth Assessment Report of the Intergovernmental Panel on Climate Change*; Cambridge university press, 2014.

(3) Reilly, J.; Prinn, R.; Harnisch, J.; Fitzmaurice, J.; Jacoby, H.; Kicklighter, D.; Melillo, J.; Stone, P.; Sokolov, A.; Wang, C. Multi-gas assessment of the Kyoto Protocol. *Nature* **1999**, *401*, 549−555.

(4) Xiao, S.; Shi, S.; Li, Y.; Ye, F.; Li, Y.; Tian, S.; Tang, J.; Zhang, X. Review on decomposition characteristics of eco-friendly gas insulating medium for high voltage gas insulated equipment. *J. Phys. D: Appl. Phys.* **2021**, *54*, 373002.

(5) Minas, S. The Paris Agreement's Technology Framework and the Need for "Transformational Change". *Carbon and Climate Law Review*; 2020; p 14.

(6) Li, Y.; Zhang, Y.; Li, Y.; Tang, F.; Lv, Q.; Zhang, J.; Xiao, S.; Tang, J.; Zhang, X. Experimental study on compatibility of eco-friendly insulating medium $C_5F_{10}O/CO_2$ gas mixture with copper and aluminum. *IEEE Access* **2019**, *7*, 83994−84002.

(7) *Novec 5110 Dielectric Fluid, Safety Data Sheet*; 3M Company: St. Paul, MN, 2021.

(8) Maiss, M.; Brenninkmeijer, C. A. M. Atmospheric SF_6: trends, sources, and prospects. *Environ. Sci. Technol.* **1998**, *32*, 3077−3086.

(9) Zhong, J.; Fu, X.; Yang, A.; Han, G.; Liu, J.; Lu, Y.; Wang, X.; Rong, M. Insulation performance and liquefaction characteristic of $C_5F_{10}O/CO_2$ gas mixture. *2017 4th International Conference on Electric Power Equipment-Switching Technology (ICEPE-ST)*; IEEE, 2017; pp 291−294.

(10) Mantilla, J. D.; Gariboldi, N.; Grob, S.; Claessens, M. Investigation of the insulation performance of a new gas mixture with extremely low GWP. *2014 IEEE Electrical Insulation Conference (EIC)*; IEEE, 2014; pp 469−473. DOI: 10.1109/eic.2014.6869432

(11) Simka, P.; Ranjan, N. Dielectric strength of C5 perfluoroketone. *Proceedings of the 19th International Symposium on High Voltage Engineering*; 2015; pp 23−28.

(12) Li, Y.; Zhang, X.; Wang, Y.; Li, Y.; Zhang, Y.; Wei, Z.; Xiao, S. Experimental study on the effect of O_2 on the discharge decomposition products of C5-PFK/N_2 mixtures. *J. Mater. Sci. Mater. Electron.* **2019**, *30*, 19353−19361.

(13) Li, Y.; Zhang, X.; Li, Y.; Wei, Z.; Ye, F.; Xiao, S.; Zhang, X.; Wang, Y. Effect of Oxygen on Power Frequency Breakdown Characteristics and Decomposition Properties of C5-PFK/CO_2 Gas Mixture. *IEEE Trans. Dielectr. Electr. Insul.* **2021**, *28*, 373−380.

(14) Guo, Z.; Tang, F.; Lv, Q.; Li, X.; Zhang, B.; Jia, S.; Huang, R. Experimental Investigation on the Arc Characteristics and Arc Quenching Capabilities of $C_5F_{10}O$-CO_2 Mixtures. *Plasma Sci. Technol.* **2019**, *6*, 231−234.

(15) Kessler, F.; Sarfert-Gast, W.; Ise, M.; Goll, F. Interaction of low global warming potential gaseous dielectrics with materials of gas-insulated systems. *Proceedings 20th International Symposium High Voltage Engineering*; 2017.

(16) Li, Y.; Zhang, X.; Xiao, S.; Chen, D.; Chen, Q.; Wang, D. Theoretical evaluation of the interaction between C5-PFK molecule and Cu (1 1 1). *J. Fluorine Chem.* **2018**, *208*, 48−54.

(17) Li, Y.; Zhang, X.; Chen, D.; Li, Y.; Zhang, J.; Cui, Z.; Xiao, S.; Tang, J. Theoretical study on the interaction between C5-PFK and Al (1 1 1), Ag (1 1 1): A comparative study. *Appl. Surf. Sci.* **2019**, *464*, 586−596.

(18) Li, Y.; Zhang, X.; Xia, Y.; Li, Y.; Wei, Z.; Wang, Y.; Xiao, S. Study on the compatibility of eco-friendly insulating gas $C_5F_{10}O/N_2$ and $C_5F_{10}O$/air with copper materials in Gas-Insulated Switchgears. *Appl. Sci.* **2021**, *11*, 197.

(19) *GB/T 528-2009 Rubber, Vulcanized or Thermoplastic—Determination of Tensile Stress−Strain Properties*; China Standard Press: Beijing, China, 2009.

(20) Muniz-Miranda, M.; Muniz-Miranda, F.; Caporali, S. SERS and DFT study of copper surfaces coated with corrosion inhibitor. *Beilstein J. Nanotechnol.* **2014**, *5*, 2489−2497.

(21) Li, Y.; Zhang, X.; Li, Y.; Chen, D.; Cui, Z.; Liu, W.; Tang, J. Interaction Mechanism between the C_4F_7N−CO_2 Gas Mixture and the EPDM Seal Ring. *ACS Omega* **2020**, *5*, 5911−5920.

(22) Nansé, G.; Papirer, E.; Fioux, P.; Moguet, F.; Tressaud, A. Fluorination of carbon blacks. An X-ray photoelectron spectroscopy study. Part II. XPS study of a furnace carbon black treated with gaseous fluorine at temperatures below 100 °C. Influence of the reaction parameters and of the activation of the carbon black on the fluorine fixation. *Carbon* **1997**, *35*, 371−388.

(23) Yamada, T.; Graham, J. L.; Minus, D. K. Density functional theory investigation of the interaction between nitrile rubber and fuel species. *Energy Fuels* **2008**, *23*, 443−450.

(24) Perdew, J. P.; Burke, K.; Ernzerhof, M. Generalized gradient approximation made simple. *Phys. Rev. Lett.* **1996**, *77*, 3865.

(25) Delley, B. An all-electron numerical method for solving the local density functional for polyatomic molecules. *J. Chem. Phys.* **1990**, *92*, 508−517.

(26) *IEC 62271-1:2007 High-voltage Switch Gear and Control Gear—Part1: Common Specifications*. 2007.